Tunneling dynamics of double proton transfer in formic acid and benzoic acid dimers

ARTICLE *in* THE JOURNAL OF CHEMICAL PHYSICS · MAY 2005

Impact Factor: 2.95 · DOI: 10.1063/1.1868552 · Source: PubMed

3 AUTHORS, INCLUDING:

Antonio Fernández-Ramos
University of Santiago de Compostela
84 PUBLICATIONS **1,813** CITATIONS
SEE PROFILE

Willem Siebrand
National Research Council Canada
201 PUBLICATIONS **5,544** CITATIONS
SEE PROFILE

Tunneling dynamics of double proton transfer in formic acid and benzoic acid dimers

Zorka Smedarchina[a)]
Steacie Institute for Molecular Sciences, National Research Council of Canada, Ottawa K1A 0R6, Canada and Department of Physical Chemistry, University of Santiago de Compostela, 15706 Santiago de Compostela, Spain

Antonio Fernández-Ramos
Department of Physical Chemistry, University of Santiago de Compostela, 15706 Santiago de Compostela, Spain

Willem Siebrand
Steacie Institute for Molecular Sciences, National Research Council of Canada, Ottawa K1A 0R6, Canada

(Received 19 November 2004; accepted 18 January 2005; published online 6 April 2005)

Direct dynamics calculations based on instanton techniques are reported of tunneling splittings due to double proton transfer in formic and benzoic acid dimers. The results are used to assign the observed splittings to levels for which the authors of the high-resolution spectra could not provide a definitive assignment. In both cases the splitting is shown to be due mainly to the zero-point level rather than to the vibrationally or electronically excited level whose spectrum was investigated. This leads to zero-point splittings of 375 MHz for $(DCOOH)_2$ and 1107 MHz for the benzoic acid dimer. Thus, contrary to earlier calculations, it is found that the splitting is considerably larger in the benzoic than in the formic acid dimer. The calculations are extended to solid benzoic acid where the asymmetry of the proton-transfer potential induced by the crystal can be overcome by suitable doping. This has allowed direct measurement of the interactions responsible for double proton transfer, which were found to be much larger than those in the isolated dimer. To account for this observation both static and dynamic effects of the crystal forces on the intradimer hydrogen bonds are included in the calculations. The same methodology, extended to higher temperatures, is used to calculate rate constants for HH, HD, and DD transfers in neat benzoic acid crystals. The results are in good agreement with reported experimental rate constants measured by NMR relaxometry and, if allowance is made for small structural changes induced by doping, with the transfer matrix elements observed in doped crystals. Hence the method used allows a unified description of tunneling splittings in the gas phase and in doped crystals as well as of transfer rates in neat crystals. © *2005 American Institute of Physics*. [DOI: 10.1063/1.1868552]

I. INTRODUCTION

Carboxylic acids tend to form dimers in which the hydroxyl group of one molecule forms a hydrogen bond with the carbonyl group of the other. The equivalence of these two hydrogen bonds allows the protons to move pairwise between the two monomers. If the motion is coherent, this should give rise to tunneling splitting in the spectra. Such a splitting has recently been observed by high-resolution spectroscopy in a cold beam of the dimers of formic[1] and of benzoic acid,[2] depicted in Fig. 1. These spectral splittings are the sum or difference of the splittings of the levels between which the transition takes place. Thus the question remains how much the initial and how much the final state of the transition contributes. In the case of formic acid, splittings were measured in a transition between the zero-point level and the first excited level of an infrared-active CO-stretching vibration.[1] The splitting in the 400 MHz range could be decomposed into two components whose magnitude differed by a factor of about 4. Experimentally it proved impossible to decide which level showed the larger splitting; nevertheless it was tentatively assigned to the excited state, based on the argument that in other systems nonhydrogenic vibrations had been shown to promote proton tunneling. In the case of benzoic acid, a splitting of the order of 1 GHz was measured in a transition between the zero-point levels of the ground state and the first singlet excited state.[2] It could not be decomposed into ground-state and excited-state components.

Another gas-phase experiment that will prove to be relevant to these observations concerns the dimer 2-pyridone/2-hydroxypyridine.[3–5] Although not a carboxylic acid dimer, it is also held together by two hydrogen bonds such that pairwise transfer of the protons of these bonds leads to an equivalent structure. As in the case of the benzoic acid dimer, a single splitting of the order of 1 GHz was observed in the transition between the zero-point levels of the ground state and the excited state.[3] This splitting was originally assigned to the excited state; following new measurements on the effect of deuterium substitution on the splitting

[a)]Electronic mail: zorka.smedarchina@nrc-cnrc.gc.ca

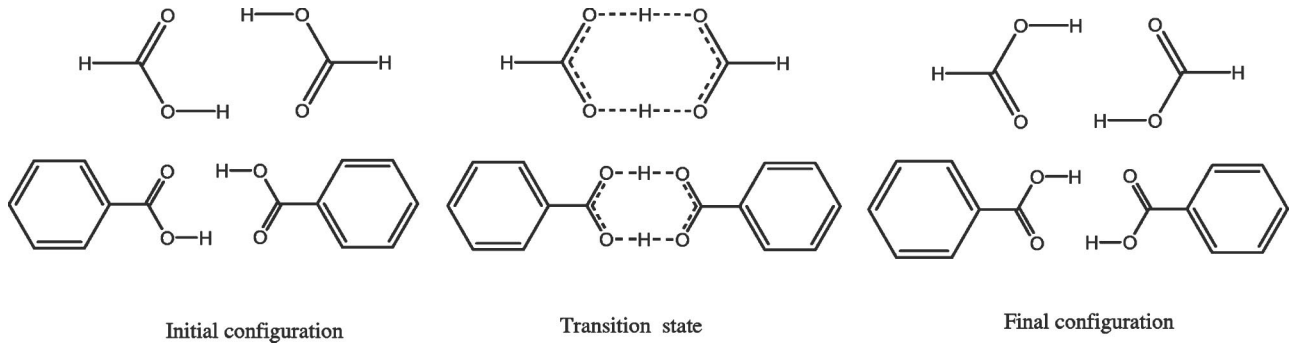

FIG. 1. Schematic representation of the double proton-transfer process in the formic and benzoic acid dimer.

and our direct dynamics calculation of the splitting in the HH, HD, DH, and DD isotopomers,[4,5] it has now been reassigned to the ground state.

Prior to these gas-phase experiments, double proton exchange in the benzoic acid dimer had been studied at length in the solid state.[6–10] The crystal structure consists of dimers, similar to those observed in the gas phase, but the low site symmetry lifts the degeneracy between the two tautomers and causes asymmetry in the tunneling potential.[11,12] The degeneracy can be approximately restored at specific sites by doping the crystal. From measurements of the proton dynamics at these sites by high-resolution laser spectroscopy, it was concluded that this dynamics reveals a proton-transfer matrix element of 6–8 GHz ($0.2–0.3\ \mathrm{cm}^{-1}$).[6,10] This implies that full restoration of the symmetry of the tunneling potential would lead to a tunneling splitting of about this value in the ground state, which should be compared with the splitting of about 1 GHz measured in the gas phase.

In this paper we use theoretical methods to account for these observations and to assign spectra whose assignment remains ambiguous. There have been earlier attempts to calculate tunneling splittings in isolated carboxylic acid dimers[13–20] but the results show wide variations and are too uncertain to solve the assignment problem. In a preliminary communication,[21] we have reported calculations of the splitting of both the zero-point level and the CO-stretching fundamental of the formic acid dimer. On the basis of these calculations and simple physical arguments, we reversed the proposed assignment of the tunneling splittings[1,20] and assigned the larger splitting of 375 MHz to the zero-point level. The calculations were based on the approximate instanton method (AIM) as implemented in the DOIT program.[4,5,22,23] They satisfactorily account for the observed splittings in this dimer as well as in the 2-pyridone/2-hydroxypyridine dimer.[4,5,21] We will use the same method to calculate the ground-state tunneling splitting in the isolated benzoic acid dimer in an attempt to assign the high-resolution spectrum.

Most of the relevant experimental data on benzoic acid concern the rate of double proton transfer in the solid, measured as reciprocal NMR spin-lattice relaxation times. These rate constants have been measured as a function of temperature for HH, HD, and DD transfers.[7,8,24] Early attempts to account for these observations were based on two-dimensional models and semiempirical parametrization.[7,25,26] The availability of new information, including gas-phase data, suggests that a new approach, based on techniques that allow integration of all the data, is timely. We therefore extend the AIM/DOIT calculations to rate constants in an attempt to relate the observed rate constants to observed tunneling splittings in these dimers.

II. TUNNELING SPLITTINGS

For reference purposes, we start with a brief summary of the AIM/DOIT procedure in the form used for tunneling in symmetric potentials. For the present purpose, we restrict ourselves to the electronic ground state. We solve the Schrödinger equation for the equilibrium configuration and the transition state along the transfer coordinate and calculate the corresponding harmonic force fields. We then combine the results to form the AIM Hamiltonian, using the transition state as the origin of the multidimensional coordinate system expressed in its (mass-weighted) normal coordinates $\{x,\mathbf{y}\}$,

$$H=\mathcal{T}+\mathcal{U},\quad \mathcal{T}=\frac{1}{2}\dot{x}^2+\frac{1}{2}\sum_{a,s}\dot{y}_{a,s}^2,$$

$$\mathcal{U}=U_{\mathrm{C}}(x)+\frac{1}{2}\sum_{a,s}\omega_{a,s}^2(y_{a,s}^2-\Delta y_{a,s}^2)-x^2\sum_{s}C_s(y_s-\Delta y_s)$$
$$-x\sum_{a}C_a(y_a\pm\Delta y_a). \qquad (1)$$

Here mode x with imaginary frequency $i\omega^*$ is chosen as the reaction coordinate and modes y_s and y_a represent symmetric and antisymmetric transverse modes, respectively, which are coupled linearly to the reaction coordinate. Since this formulation identifies the reaction coordinate as the mode with imaginary frequency throughout the reaction, the other active modes, which remain by definition transverse modes throughout, can be treated in an approximate way that keeps the treatment tractable for large systems. The assumed linearity of the coupling of the reaction coordinate to the transverse modes implies that these modes, which are treated as independent harmonic oscillators, will be only displaced during the tunneling. The quantum-chemically calculated displacements are used as a measure of the coupling strength. The antisymmetric modes have the same symmetry as the tunneling mode and thus are displaced between the (equivalent) initial and final equilibrium configurations. The sym-

metric modes do not undergo such reorganization and may only be displaced between the equilibrium configuration and the transition state. The kinetic-energy operator is taken to be diagonal.

The one-dimensional potential along the tunneling coordinate, represented by $U_C(x)$ in Eq. (1), is a "crude-adiabatic" potential evaluated with the heavy atoms fixed in the equilibrium configuration, i.e., with $y_a = \pm \Delta y_a$, $y_s = \Delta y_s$; it is equivalent to the potential along the linear reaction path (LRP). This symmetric double-minimum potential has a maximum U_0 at $x=0$, minima (=0) at $x = \pm \Delta x$, and curvatures in the minima and at the top given by the effective frequency ω_0 and the imaginary frequency ω^*, respectively. All parameters are evaluated directly from the output of standard quantum-chemical structure and force field calculations at the two stationary configurations. In the present study we use a potential based on the calculated values of Δx, U_0, and ω_0. For the shape of the potential in the intermediate points we use a quartic potential of the form

$$U_C(x) = U_0[1 - (x/\Delta x)^2]^2, \tag{2}$$

which can be shown to be a valid approximation for the present purpose. In the harmonic approximation, the coupling coefficients $C_{a,s}$ in Eq. (1) are restricted to linear terms in the transverse mode displacements and are given by

$$C_a = \omega_a^2 \Delta y_a / \Delta x, \quad C_s = \omega_s^2 \Delta y_s / \Delta x^2. \tag{3}$$

To treat the tunneling dynamics governed by such a Hamiltonian, the transverse modes are separated into "high-frequency" (HF) modes, treated adiabatically, and "low-frequency" (LF) modes, treated in the sudden approximation, according to the value of the "zeta factor"[27]

$$\zeta_{a,s} = \frac{\omega_{a,s}}{\sqrt{\Omega^2 - C_{a,s}^2/2\omega_{a,s}^2}}, \tag{4}$$

where Ω, the "scaling" frequency, is defined by $\Omega^2 \Delta x^2 = U_0$, $U_0 \equiv U_C(0)$ being the crude-adiabatic barrier height. Modes are treated as HF or LF depending on whether $\zeta_{a,s} > 1$ or <1. Modes for which $\zeta_{a,s} \sim 1$ require special treatment and will be dealt with when the need arises.

Coupling to HF modes leads to an effective one-dimensional motion with renormalized potential $U_C^{\text{eff}}(x)$ and coordinate-dependent mass $m^{\text{eff}}(x)$. Since each HF mode y_i is assumed to follow the reaction coordinate x adiabatically, we have $\partial \mathcal{U} / \partial y_i = 0$, so that $y_s^{\text{HF}} = C_s x^2 / \omega_s^2$ and $y_a^{\text{HF}} = C_a x / \omega_a^2$. Substitution in the Hamiltonian (1) provides a correction to the mass of the tunneling particle and thus modifies the kinetic-energy operator,

$$\mathcal{T}^{\text{eff}} \equiv \frac{1}{2}\dot{x}^2 + \frac{1}{2}\sum_{a,s}^{(\text{HF})} \dot{y}_{a,s}^2 = \frac{1}{2} m^{\text{eff}}(x) \dot{x}^2. \tag{5}$$

Using Eq. (3), we obtain for the dimensionless renormalized mass

$$m^{\text{eff}}(x) = 1 + (x/\Delta x)^2 \sum_s^{(\text{HF})} \Delta m_s + \sum_a^{(\text{HF})} \Delta m_a,$$
$$\Delta m_s = (2\Delta y_s^{\text{HF}}/\Delta x)^2, \quad \Delta m_a = (\Delta y_a^{\text{HF}}/\Delta x)^2. \tag{6}$$

Renormalization of the one-dimensional potential (2) yields

$$U_C^{\text{eff}}(x) = U_{0,\text{VA}}^{\text{HF}}[1 - (x/\Delta x)^2]^2, \tag{7}$$

i.e., a potential of the same shape and width as Eq. (2) but with a barrier height corrected by the standard vibrational-adiabatic correction for the HF modes only.

Because at $T=0$ the energy equals zero along the instanton path, the corresponding one-dimensional action is given by[4]

$$S_I^0(0) = \frac{2}{\hbar} \int_{-\Delta x}^{\Delta x} dx \sqrt{2 m^{\text{eff}}(x) U_C^{\text{eff}}(x)}. \tag{8}$$

The effect of the LF modes can be shown[4] to take the form of corrections to this one-dimensional action, which in the absence of anharmonic couplings lead to a multidimensional action of the form

$$S_I(0) = \frac{S_I^0(0)}{1 + \sum_s^{(\text{LF})} \delta_s(0)} + \alpha \sum_a^{(\text{LF})} \delta_a(0). \tag{9}$$

The δ_a terms of the form[22,23]

$$\delta_a(0) = (2C_a \Delta x)^2 / \omega_a^3 \tag{10}$$

lead to a Franck–Condon factor arising from the reorganization of antisymmetric LF modes, which act similarly to a thermal heat bath. Symmetric LF modes, represented by δ_s terms of the form[22,23]

$$\delta_s(0) = \frac{\omega_0}{\omega_s} \left(\frac{C_s \Delta x^2}{2U_0} \right)^2 \tag{11}$$

effectively reduce the tunneling distance and thus enhance tunneling; the factor $\alpha < 1$ in Eq. (9) is the square of this reduced distance (in dimensionless units).[5]

To account for the preexponential factor in the instanton expression for the zero-point tunneling splitting,[4] the one-dimensional action (8) is replaced by $S_I^0(E_0)$, the action evaluated at the zero-point energy $E = E_0$ rather than at $E = 0$ with a potential of the type (7) but a barrier height $U_{0,\text{VA}}$, which is now vibrationally adiabatic over *all* modes. The final expression for the zero-point splitting in AIM thus assumes the form

$$\Delta_0 \equiv \Delta(v=0) = \frac{\omega_0}{\pi} \exp\left\{ -\frac{1}{2}\left[\frac{S_I^0(E_0)}{1 + \sum_s^{(\text{LF})} \delta_s(0)} + \alpha \sum_a^{(\text{LF})} \delta_a(0) \right] \right\}. \tag{12}$$

For the dimers under consideration all these parameters will be evaluated from standard quantum-chemical codes for structures and force fields at the stationary configurations, i.e., the equilibrium configuration and the transition state.

III. RATE CONSTANTS

Tunneling splittings can be observed only when the initial and final states are in resonance so that the forward and backward reactions are in phase. This implies a double-minimum (or multiple-minimum) potential that is symmetric or nearly so, such that the difference between the minima of the two wells is smaller than the coupling between the wells. This energy difference enters the ratio of the rates of the forward and backward reaction as a Boltzmann factor and thus affects their phase relationship. If it is large, the tunneling splitting vanishes and the dynamics of the system can only be represented by a reaction rate or, more restrictively, by a first-order rate constant associated with a reaction that proceeds exponentially in time. In the present context, the need to compare rate constants and tunneling splittings arises if one wants to relate the proton dynamics of dimers in the gas phase and in a matrix. It also arises if theoretical methods designed for rate processes are used to calculate tunneling splittings.

In the carboxylic acid crystals under consideration the basic units are dimers. As a result of the low site symmetry, the two tautomers related by the double proton exchange are not completely equivalent in the crystal and the double-minimum potential shows a small asymmetry. The protons are still mobile within each dimer, but instead of a tunneling splitting one observes a rate process. In the benzoic acid crystal, it has been possible to reduce this asymmetry by doping and to derive values for the effective tunneling splitting as a function of the residual asymmetry. It is therefore of interest to compare the tunneling splitting in isolated dimers and doped crystals with the rate constants observed in doped and neat crystals.

The instanton method expresses the rate constant for proton transfer at $T=0$ in the form

$$k(0) = \frac{\omega_0}{2\pi} e^{-S_I(0)} = \frac{\pi}{2\omega_0}\Delta_0^2, \tag{13}$$

where $S_I(0)$ is given by Eq. (9) and Δ_0 by Eq. (12). Unfortunately, this formula cannot be used directly to relate low-temperature rate constants observed in solids to tunneling splittings in the gas phase or even in doped crystals since the perturbation imposed by the solid environment is generally far from weak and may also be affected by dopants. To calculate the corresponding rate constants, it will thus be necessary to adapt the parameters of the model to the crystal environment.

Since rate constants are usually measured as a function of temperature, we need to generalize our equation to nonzero temperatures. This implies a nonzero probability of the protons to transfer over rather than through the barrier. In the instanton formalism, subject to a temperature constraint discussed below, these two paths appear as contributions of two extrema of the Euclidean action to the rate of decay of a metastable state, one corresponding to the transition state and the other to a periodic orbit called instanton. The rate constant thus consists of a "classical" and a "tunneling" component. The classical, over-barrier component is calculated from standard transition state theory (TST). The tunneling component is proportional to $e^{-S_I(T)}$, where $S_I(T)$, the multidimensional instanton action at nonzero temperature, is written as a direct generalization of Eq. (9),

$$S_I(T) = \frac{S_I^0(T)}{1+\sum_s^{(\mathrm{LF})} \delta_s(T)} + \alpha \sum_a^{(\mathrm{LF})} \delta_a(T). \tag{14}$$

Here $S_I^0(T)$ is the instanton action of the effective one-dimensional motion found via periodic-orbit calculations.[22,23] For systems with very small asymmetry, the temperature dependence of the correction terms is of the form[22,27]

$$\delta_a(T) = \delta_a(0)\tanh\frac{\hbar\omega_a}{4k_BT} \tag{15}$$

and

$$\delta_s(T) = \delta_s(0)\coth\frac{\hbar\omega_s}{2k_BT}. \tag{16}$$

At nonzero temperatures, the rate constant then takes the form

$$k(T) = k_{\mathrm{TST}}(T) + \frac{\omega_0}{2\pi} e^{-S_I(T)}, \tag{17}$$

where $S_I(T)$ is given by Eq. (14). As mentioned earlier in this paragraph, this formula is subject to a temperature constraint. It should not be used above the crossover temperature T^* defined by

$$T^* = \hbar\omega^*/2\pi k_B, \tag{18}$$

where the instanton ceases to exist, so that the tunneling term as formulated in Eq. (17) is no longer appropriate. At temperatures $T\sim 2T^*$ and higher, the tunneling contribution tends to be negligible relative to the classical contribution, so that the rate constant converges to $k_{\mathrm{TST}}(T)$.

In the solid, the dimers are subject to van der Waals forces, which compress the hydrogen bonds and thus modulate the transfer distance (and thus also the barrier height). This results in a static as well as a dynamic effect on the tunneling rate. In terms of Eq. (14), the static effect, i.e., the reduction of the transfer distance, enters through $S_I^0(T)$, the one-dimensional instanton action. It follows from Eq. (8) that this action varies quadratically with the transfer distance. To show this we rewrite this equation in terms of $\xi = x/\Delta x$ and neglect the relatively weak effect of the Δx dependence of the tunneling mass,

$$S_I^0(0) = \frac{2\Delta x\sqrt{2m_0U_0(\Delta x)}}{\hbar}\int_{-1}^{1}\Phi(\xi)d\xi, \tag{19}$$

where $\Phi(\xi)$ is a line shape function that is independent of Δx. For any symmetric barrier, U_0 is a quadratic function of the tunneling coordinate and thus of the barrier width. It follows that for small variations in the barrier width, $S_I^0(0)$ will depend quadratically on this width and thus on the transfer distance r. This allows us to calculate the one-dimensional instanton action in the solid from that in the gas phase by the expression

$$(S_I^0)_{\text{solid}} = (S_I^0)_{\text{gas}}(r_{\text{solid}}/r_{\text{gas}})^2 \equiv (S_I^0)_{\text{gas}}\rho, \tag{20}$$

ρ being the appropriate compression factor, which applies equally to the barrier height and thus also to the rate constant and the tunneling splitting since

$$\ln k(0) = \ln(\pi/2\omega_0) + 2\ln\Delta_0(r) = Br^2 + \text{const}. \tag{21}$$

The dynamic effect of the lattice on the transfer rate enters through the contribution of lattice modes to $\Sigma_s\delta_s(T)$, which increases the transfer rate, and to $\Sigma_a\delta_a(T)$, which decreases it. Only the latter effect is included if the lattice phonons are treated as a thermal heat bath that provides friction. However, in the system at hand such an effect is expected to be relatively weak, since the protons move inside the dimer so that their motion is not directly affected by antisymmetric lattice vibrations. The main coupling between the tunneling mode and lattice vibrations is expected to occur through compression of hydrogen bonds, an effect associated with symmetric lattice vibrations in which a given dimer is squeezed by neighboring dimers that move in opposite directions. Coupling of the tunneling mode to these symmetric lattice modes gives rise to an effective reduction of the tunneling distance. The effect of these modes on the transfer rate is the dynamic complement of the static compression represented by Eq. (20). In the AIM formalism it is included by the addition of a symmetric correction terms $\delta_s^{\text{lattice}}(T)$ to the sum in the denominator of Eq. (14).

To keep the treatment tractable, we restrict ourselves to the leading new terms in this sum, i.e., the terms corresponding to lattice modes in which a dimer *X*, located between two dimers *Y* in a quasilinear array *Y*-*X*-*Y* along the tunneling direction, is squeezed by symmetric *XY*-stretching motions. This contribution will be proportional to the squared amplitude of these modes, which can be obtained from their effective mass *M* and frequency ω,

$$A^2(T) = A^2(0)\coth\frac{\hbar\omega}{2k_BT}, \tag{22}$$

where $A^2(0)=\hbar/M\omega$ is the zero-point amplitude. The corresponding value of $\delta_s^{\text{lattice}}(T)$ is derived from the observation that the most strongly coupled lattice modes will be parallel to the most strongly coupled intradimer modes, such as the symmetric O···O stretch vibrations. In that case the $\delta_s^{\text{lattice}}(T)$ values will be proportional to the square of the vibrational amplitudes,

$$\delta_s^{\text{lattice}}(T) = \delta_s^{\text{dimer}}(0)\left[\frac{A_s^{\text{lattice}}(0)}{A_s^{\text{dimer}}(0)}\right]^2\coth\frac{\hbar\omega}{2k_BT}. \tag{23}$$

We apply a similar approach to estimate the additional Franck–Condon factor of the form $\exp(-\alpha\delta_a^{\text{lattice}}(T))<1$ by which the phonon bath hinders proton transfer. From Eqs. (15) and (23) the effect of coupling to antisymmetric phonons is given by

$$\delta_a^{\text{lattice}}(T) = \delta_a^{\text{dimer}}(0)\left[\frac{A_a^{\text{lattice}}(0)}{A_a^{\text{dimer}}(0)}\right]^2\tanh\frac{\hbar\omega}{4k_BT}. \tag{24}$$

The terms (23) and (24) are added to the corresponding sums of Eq. (14) for processes in crystals.

IV. FORMIC ACID DIMER

A. Tunneling splitting in the gas phase

Madeja and Havenith[1] observed two tunneling splittings in the high-resolution infrared spectrum of a CO-stretch fundamental of the formic acid dimer isolated in a cold beam: one splitting associated with the zero-point level and the other with the excited level. However, they were unable to ascertain which splitting belonged to which level. Since the two splittings differ by a factor of about 4, this problem should be solvable if we can establish what will be the effect of excitation of the infrared-active C–O stretching mode on the transfer probability. Since the reaction coordinate is *gerade* but the infrared-active mode is obviously *ungerade* in the centrosymmetric dimer, there can be no Dushinsky-type mixing between these modes in the harmonic approximation, i.e., in a transfer potential constructed from stationary configurations that contain only terms linear and quadratic in the vibrational coordinates. Hence in this approximation, the tunneling splitting of the CO-stretch fundamental is predicted to be the same as that of the zero-point level. Since this is not the case, the harmonic approximation is clearly inadequate; there must be at least one other mode involved to generate a coupling of the appropriate symmetry, which thus requires minimally a term that is cubic in the vibrational coordinates.

The transition state of the formic acid dimer, depicted in Fig. 1, belongs to the D_{2h} point group. Apart from the reaction coordinate b_{3g}, characterized by an imaginary frequency, there are 23 normal modes, nine symmetric (a_g), seven antisymmetric (b_{3g}), i.e., with the same symmetry as the reaction coordinate, and seven asymmetric modes. The asymmetric modes, which include the infrared-active CO-stretch mode b_{1u}, cannot contribute to the tunneling in the harmonic approximation. However, pairs of such modes can contribute to anharmonic coupling if their direct product transforms as b_{3g}. Thus the b_{1u} mode can contribute in this way if it is paired with a b_{2u} mode.

There are good reasons to suspect that the additional mode is a C═O stretching vibration. Double proton transfer transforms the C–O modes into C═O modes and vice versa. It is reasonable to assume that this transformation of the dimer structure will act as a drag on the tunneling. Formally, this follows from the observation that these modes have frequencies that fit the HF criterion; hence the interaction should be included adiabatically and thus it increases the effective mass of the tunneling mode. The effect increases with the degree of excitation of the modes involved; therefore, it seems likely that the tunneling splitting of the CO-stretch fundamental will be *smaller* than that of the zero-point level. This is quantitatively confirmed by our direct dynamics calculations.[21]

These calculations were based on potential-energy surfaces evaluated at two levels of quantum chemistry: DFT-B3LYP/6-31+G(*d*) and, more elaborately, MCG3//MC-QCSD/3 (i.e., MC-QCISD/3 with single-point energies evaluated at the MCG3 level).[21,28] In Table I we compare the rotational constants resulting from these and other calculations with the experimental values reported by Madeja and

TABLE I. Rotational constants of $(DCOOH)_2$ in cm^{-1}.

Source	*A*	*B*	*C*
Observed[a]	0.202 05	0.070 585	0.052 373
Observed[b]	0.199 91	0.069 79	0.051 73
Calculated[c]	0.202 0	0.069 4	0.051 7
Calculated[d]	0.201 6	0.084 1	0.059 3
Calculated[e]	0.201 5	0.070 9	0.052 5

[a]Reference 1, high-resolution spectrum.
[b]Reference 30, electron diffraction.
[c]This work, B3LYP/6-31+G(*d*) level.
[d]This work, MCG3//MC-QCSD/3 level.
[e]Reference 29, MP2/TZ2P level.

Havenith.[1] It follows that the MCG3 results are superior to the B3LYP results and roughly on a par with the MP2/TZ2P results reported by Neuheusser *et al.*[29] However, the calculated O···O distances, listed in Table II differ by 0.03 Å between the MCG3 (2.702 Å) and MP2/TZ2P (2.672 Å) results. An intermediate value of 2.696 Å has been obtained by electron diffraction.[30] The zero-point splitting for $(DCOOH)_2$ calculated at the MCG3 level amounts to 441 MHz. Since we assign the larger of the observed splittings, which equals 375 MHz, to the zero-point level, it follows that the MCG3-level calculation represents the splitting satisfactorily. The B3LYP potential yields a zero-point splitting of 510 MHz, which is less accurate but still acceptable as a first approximation. The calculated splittings for the excited CO-stretch level were 163 for B3LYP and 129 for MCG3 compared to an observed splitting of 94 MHz.

To extend the calculations to dimers deuterated at one or both carboxyl groups, we have to take account of the fact that the zeta factors (4) increase upon deuteration. As a result, more of the coupled modes need to be treated in the adiabatic approximation. This is the case for the most strongly coupled symmetric mode, which represents O···O stretching, in the case of DD transfer. This increases the deuterium isotope effect. In the case of HD transfer, this coupled mode falls in between the HF and LF categories. Therefore we have chosen to represent its tunneling splitting by the geometric mean of the splittings calculated with an HF and a LF assignment of this mode, the same *hybrid* approach we adopted earlier for HD tunneling splitting in the 2HP/2PY dimer.[5] All results are collected in Table III.

TABLE II. Principal parameters of the hydrogen bonds relevant to the dynamics of double proton transfer in the benzoic and formic acid dimer. Distances in angstroms, angles in degrees, energies in kcal/mol. Numbers without reference are obtained in the present work at the B3LYP/6-31+G(*d*) level and (printed in italics) at the MCG3//MC-QCSD/3 level. Experimental numbers are printed in bold.

	Benzoic		Formic
	Gas phase	Solid state	Gas phase
R_{O-O}	**2.702**[a]	**2.608**[b]	**2.696**[c]
	2.715[d]	**2.64**[a]	2.672[e]
	2.69[f]	2.561[d]	2.707[g]
			2.72[f]
	2.688		2.718
			2.702
R_{O-H}	1.022[d]	**0.995**[b]	**1.033**[h]
			0.995[g]
	1.004		1.003
			0.991
∠O–H–O			**180**[h]
			178.9[g]
	179.5		176.8
			179.1
Transfer distance *r*	0.680	**0.625**[b]	0.713
	0.687[i]		*0.720*
LRP barrier height U_0	21.43		24.62
			27.58
Adiabatic barrier height U_A	7.33		8.38
			7.94

[a]Reference 36.
[b]Reference 11.
[c]Reference 30.
[d]Reference 37.
[e]Reference 29.
[f]Reference 20.
[g]Reference 31.
[h]References 30 and 38.
[i]See Sec. V C.

B. Rate constant calculations

No experimental data are available for the rate of proton transfer in the formic acid dimer. Although it seems doubtful whether such data will become available in the near future, we report such calculations here to allow comparison with rate constant calculated by Kim[31] and Tautermann *et al.*[32] Kim reported rate constants for double proton and double deuteron transfer in the gas phase at temperatures $T \geqslant 200$ K. These calculations were based on TST with semiclassical tunneling corrections with a potential-energy surface evaluated with extended Gaussian-2 theory ($G2^*$). The more recent calculations of Tautermann *et al.*[32] also used TST with tunneling corrections but employed more elaborate quantum-chemical methods and a wider temperature range ($T \geqslant 100$ K). However, they concluded that the potential obtained at the modest B3LYP/6-31+G(*d*) level reproduces the high-level results quite well, a conclusion supported by our own results for tunneling splittings.

Since our results refer to zero temperatures, they are not directly comparable to these high-temperature rate constant calculations. To allow a comparison between our method and the TST approach, we have to extend our AIM/DOIT calculations to nonzero temperatures. While the low-temperature rate constants follow directly from the zero-point tunneling splittings, straightforward extensions of these calculations to higher temperatures would lead to a loss of accuracy. As shown in earlier publications,[27] the AIM Hamiltonian can be formulated in two equivalent ways, with the one-dimensional tunneling potential being represented by either a crude-adiabatic or an adiabatic potential. Although nominally equivalent, the various approximations used introduce differences, which favor the crude-adiabatic formulation for the lowest temperatures, where the tunneling trajectory is close

TABLE III. Main dynamics parameters of the AIM/DOIT calculations for the benzoic and formic acid dimer calculated at the B3LYP/6-31+G(*d*) level.

	Benzoic			Formic		
	HH	DD	HD	HH	DD	HD
U_0^{eff} (kcal/mol)	16.57	13.14	16.90	19.85	17.36	19.87
Δx (Å amu$^{1/2}$)	0.585	0.794	0.683	0.588	0.794	0.688
ω^* (cm^{-1})	1255	923	1083	1320	977	1141
ω_0 (cm^{-1})	2749	1996	2398	2817	2057	2456
$\delta_s(0)/\Delta m_s$	0.32/0.10	0.26/0.81	0.36/0.14	0.32/0.21	0.34/0.63	0.38/0.12
$\alpha\delta_a(0)/\Delta m_a$	3.31/0.02	6.65/0	3.24/0.03	3.26/0.23	4.86/0.20	3.04/0.23
Zero-level splitting						
Δ_0 (cm^{-1})	6.4×10^{-2}	4.1×10^{-4}	5.5×10^{-3}	1.9×10^{-2}	2.2×10^{-4}	2.5×10^{-3}
Δ_0 (MHz)	1920	12	166	560	6.5	74

to linear, and the adiabatic formulation for higher temperatures, where this trajectory approaches the minimum-energy path. The implications of the zeta factor (4) change accordingly such that LF modes in the crude-adiabatic formulation may become HF modes in the adiabatic formulation, which for still higher temperatures joins smoothly with TST. If the mode has a low ζ factor, the two formulations will yield similar results. If the mode has a high ζ factor, it must always be treated adiabatically. But if the mode has a ζ factor close to unity, ambiguities arise. To calculate corresponding rate constants at higher temperatures, the most prudent approach would be to use the adiabatic formulation. Where appropriate, an interpolation scheme has been used. More details about this procedure are presented in Sec. V E.

The calculations are based on the transfer potentials previously evaluated at both the B3LYP and the MCG3 level.[21] The latter level, which yields an adiabatic barrier height $U_A=7.93$ kcal/mol is comparable to the highest level used by Tautermann *et al.*,[32] for which $U_A=7.90$ kcal/mol. By contrast, the corresponding G2* value of Kim[31] equals 8.94 kcal/mol. In Fig. 2 our results are compared with those reported in Ref. 32. Although we obtain comparable rate constants for HH transfer, our rate constants for DD transfer are considerably lower, leading to larger isotope effects. For instance at 200 K our isotope effect is calculated to be 174, while that in Ref. 32 equals 18.5 and that in Ref. 31, admittedly calculated with a somewhat higher barrier, equals 139. At 100 K, our isotope effect is more than two orders of magnitude larger than that of Ref. 32. Together with the authors' recognition[33] that their earlier high-level calculation on malonaldehyde underestimated the isotope effect on the tunneling splitting, these results suggest that their isotope effects are not correct. We return to these data in Sec. V E. after discussing kinetic isotope effects observed in benzoic acid crystals.

V. BENZOIC ACID DIMER

A. Tunneling splitting in the gas phase

Remmers, Meerts, and Ozier[2] used high-resolution ultraviolet spectroscopy to investigate the rotationally resolved excitation spectrum of the first singlet-singlet transition ($S_1 \leftarrow S_0$)) of the benzoic acid dimer. They found two overlapping components separated by 1107 ± 7 MHz, the separation which they assigned convincingly to the difference in tunneling splitting between the ground state and the excited state. This splitting exceeds that observed for the formic acid dimer by a factor of about 3. In the excited state of the benzoic acid dimer the excitation is essentially localized on one of the monomers. Theoretically, one expects the ground state to be planar and the excited state to be bent, since excitation reduces the acidity of the monomer, so that the two hydrogen bonds will no longer be equivalent. The spectra confirm this expectation and indicate weaker hydrogen bonding as a result of the excitation.[2]

This weaker bonding in the excited state immediately suggests that the ground state will have the larger splitting. The larger skeletal reorganization accompanying tunneling in S_1 compared to S_0 is consistent with this suggestion, as is the inequivalence of the two hydrogen bonds in S_1, since the weaker hydrogen bond is likely to have the larger effect on

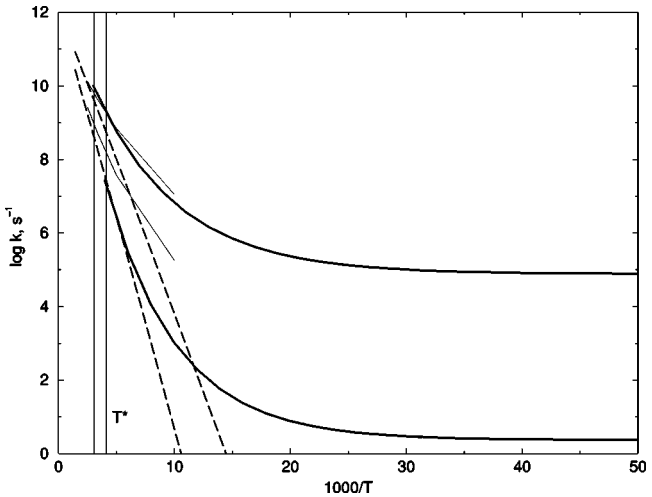

FIG. 2. Arrhenius plot of the rate constants for HH and DD transfers in isolated formic acid dimers. The thick solid lines represent our AIM/DOIT calculations based on MCG3-level potentials and the thin solid lines represent TST calculations with semiclassical tunneling corrections reported in Ref. 32. The broken lines represent our classical TST calculations for the MCG3 potential. The left and right vertical lines denote, respectively, HH and DD crossover temperatures, defined by Eq. (18).

the transfer. The situation is analogous to that in the 2-pyridone/2-hydroxypyridine dimer,[3–5] where the effect of selectively deuterating one of the two inequivalent hydrogen bonds leads to a stronger reduction of the splitting for the weaker bond. In fact it is quite possible that the weakening of one of the hydrogen bonds compromises the coherence of the transfer to such an extent that the tunneling splitting in the excited state is negligible. For these reasons we assign the observed splitting, or at least most of it, to the ground state.

To probe this assignment, we carried out AIM/DOIT calculations for the ground state. In view of the size of this dimer, the calculation of the potential-energy surface for the tunneling is restricted to the B3LYP/6-31+G(*d*) level, which has proved to be acceptable for the formic acid dimer. As before,[21] we used the GAUSSIAN98 suite of programs.[34] A single transition state was found indicating concerted transfer, in agreement with the observed tunneling splitting. The Hamiltonian for the benzoic acid dimer has 84 vibrational degrees of freedom. Apart from the reaction coordinate, the transition state has 14 symmetric, 42 antisymmetric, and 27 asymmetric vibrational modes. In Table II the principal parameters for the tunneling potential are compared with those of the formic acid dimer obtained at the same level of theory. The hydrogen bonding, as reflected in the O···O distance and O–C–O angle as well as in the adiabatic barrier height, is slightly stronger for the benzoic acid dimer. These effects combine to yield substantially different linear reaction paths, characterized by tunneling distances $r=0.713$ and 0.680 Å, with corresponding crude-adiabatic barrier heights $U_0=24.62$ and 21.43 kcal/mol for formic and benzoic acid dimers, respectively.

With these parameters as direct input into the DOIT 2.0 code we calculate a zero-point tunneling splitting of 1920 MHz, which is a factor of about 1.7 larger than the observed value of 1107 MHz. In the formic acid dimer the splitting of 510 MHz calculated at the same level is also larger than the observed splitting of 375 MHz, namely, by a factor of about 1.4. Both factors probably reflect the tendency of the B3LYP potential to underestimate the barrier height and width. From this result, we therefore conclude that the calculations are consistent with a splitting dominated by the ground state with a small or negligible contribution from the excited state.

A detailed look at the tunneling mechanisms in the two dimers indicates their essential similarity. In both cases the net effect of coupling between the tunneling mode and transverse modes, represented by Eq. (9), is a more than 20-fold increase in the tunneling splitting. While in the benzoic acid dimer the couplings are distributed over more modes, as expected for a larger system, their sums are basically the same in the two dimers. Some of the modes with a strong effect on the splitting are depicted in Fig. 3 and listed in Table IV. Note that the mode descriptions in the first column have only qualitative significance, the listed motions being generally mixed with other motions. The modes listed are selected on the basis of the large $\delta_{a,s}$ values, not on the basis of their nominal character.

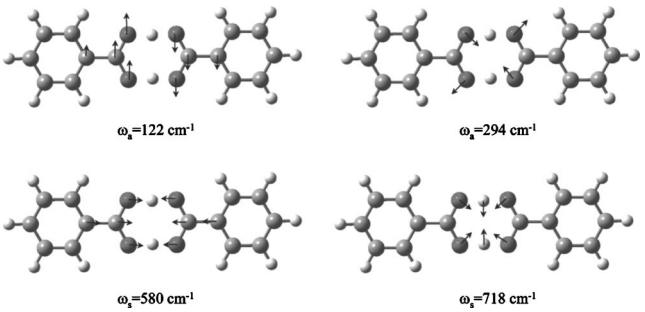

FIG. 3. Two antisymmetric (top) and two symmetric modes that are strongly coupled to the tunneling mode in the benzoic acid dimer.

B. Deuterium isotope effects

Calculations are also reported for dimers in which one or both of the carboxyl groups are deuterated. The results, collected in Table III, predict a tunneling splitting of 12 MHz for the DD and 160 MHz for the HD isotopomer. According to Eqs. (6) and (8), increasing the tunneling mass will mainly affect the one-dimensional action S_I^0. Since the HD mass is the average of the HH and DD masses, the tunneling splitting for HD transfer is expected to be close to the geometric mean of the tunneling splittings for HH and DD transfers. The calculated splittings agree with this expectation. Since the barrier is narrower and lower for the benzoic acid than for the formic acid dimer, the deuterium isotope effect on the splitting is smaller.

C. Tunneling splitting in doped crystals

In the benzoic acid crystal the hydrogens move in an asymmetric potential with a difference of about 60 cm^{-1} between the minima.[6,24] However, doping the crystal with thioindigo (or selenoindigo), the molecules which replace a benzoic acid dimer in the lattice, reduces this difference to a value small enough to allow indirect observation of low-temperature tunneling splitting for dimers adjacent to the dopant. Using high-resolution laser spectroscopy, Trommsdorff and co-workers[6,10] measured a zero-temperature tunneling matrix element $J=8.4\pm1$ GHz (6.5 ± 1.5 for selenoindigo). We take this value as a rough measure of the tunneling splitting for zero asymmetry.

It should be compared with the splitting of 1.1 GHz observed in the isolated dimer. As discussed earlier, in addition to intradimer interactions, the tunneling dynamics in crystals is subject to three types of effects of the environment: a (static) compressing effect on the O···O distance, an (dynamic) effect of coupling to "symmetric" lattice phonons, which will increase the splitting, and an (dynamic) effect of coupling to "antisymmetric" lattice phonons (phonon bath) resulting in a Franck–Condon factor smaller than unity, which will reduce the splitting. The significantly larger value of the tunneling splitting in the crystal indicates therefore that the effect of the phonon bath is smaller than the effects of the other couplings, in agreement with the expectation that proton exchange inside the dimer is partly screened from such bath effects. This is further confirmed by the good agreement between the experimental and calculated transfer rates in pure crystals discussed in the following section.

TABLE IV. Main dynamics parameters of the modes most active in the dynamics of double proton transfer in the benzoic and formic acid dimers calculated at the B3LYP/6-31+G(*d*) and the MCG3//MC-QCSD/3 level, respectively. The modes of the benzoic acid dimer are depicted in Fig. 3. The mode description is approximate, as the active modes mix between the stationary structures.

	Frequency (symmetry)		Effect		
Mode description	Ground state	Transition state	$S_I(0)$	$\delta_s(0)$	$\alpha\delta_a(0)$
Benzoic					
Reaction coordinate	3107 (a_g)	1255*i* (b_{3g})	20.69		
O···O stretching	426 (a_g)	580 (a_g)		0.15	
OCO bending	665 (a_g)	718 (a_g)		0.11	
COH bending component	105 (a_g)	122 (b_{3g})			0.92
CCO in-plane bending	238 (a_g)	294 (b_{3g})			1.30
Formic					
Reaction coordinate	3282 (a_g)	1430*i* (b_{3g})	25.85		
O···O stretching	200 (a_g)	521 (a_g)		0.28	
OCO bending	681 (a_g)	750 (a_g)		0.07	
CCO in-plane bending	164 (a_g)	224 (b_{3g})			1.06

The reduction of the O···O distance in the dimer units caused by crystal forces can be assessed from neutron diffraction data[11] which lead to a transfer distance $r^{\text{solid}}=0.625$ Å at 20 K. No experimental value is available for the gas-phase dimer and the theoretical values are based on calculations performed at a relatively low level, as listed in Table II. In our calculations we use the transfer distance $r^{\text{gas}}=0.687$ Å obtained from the B3LYP/6-31+G(*d*) value of 0.680 Å after scaling by a factor of 1.01 obtained from a comparison of B3LYP and MCG3//MC-QCSD/3 results for the formic acid dimer. The ratio $\rho=(r^{\text{solid}}/r^{\text{gas}})^2=0.83$ thus found yields the compression factor in Eq. (20).

While in the formic acid dimer the symmetric coupling to LF modes is dominated by a single O···O stretching mode, in the benzoic acid dimer this coupling is distributed over three such modes. We therefore include three symmetric lattice vibrations in the calculation, namely, the three lattice modes that are parallel to these intradimer modes, and calculate their δ_s values by the procedure outlined in Sec. III. We take the effective mass of these lattice modes to be equal to the mass of a benzoic acid molecule, viz., 122, and the frequency equals the Debye frequency divided by the square root of 2, viz., 85 cm^{-1}. From Eq. (23) we then obtain values $\Sigma_{s=1}^{3}\delta_s^{\text{lattice}}(0)$ of 0.13 for HH, 0.15 for HD, and 0.18 for DD. In a similar manner we estimate the Franck–Condon factor related to coupling with antisymmetric phonons. We take the effective mass of these modes to be that of the dimer molecule, and the frequency again to be 85 cm^{-1}. From Eq. (24) we then obtain a value for $\Sigma_a\delta_a^{\text{lattice}}(0)$ of the order 0.2–0.3, which, as expected, is much smaller than the corresponding intradimer counterpart listed in Table III. If we add the new coupling terms $\Sigma_s\delta_s^{\text{lattice}}(0)$ and $\Sigma_a\delta_a^{\text{lattice}}(0)$ to Eq. (9), and use the observed transfer distance of 0.625 Å for neat crystals, we obtain a tunneling splitting of about 17 GHz, i.e., about twice the reported value $J=8.4\pm1$ for crystals doped with thioindigo.[6] A decrease in the δ_s values for the lattice modes by a factor of 2 would decrease the calculated splitting by about 20%.

D. Rate constants in doped crystals

Low-temperature rate constants measured in crystals doped with thioindigo[35] lead to an estimate $k(0)\leqslant 10^7\ \text{s}^{-1}$. We can use this low-temperature limit to check relation (13). Substituting the calculated value of ω_0 and the splitting implied by the high-resolution measurements, we obtain for HH transfer a rate constant of $k(0)=0.85\times10^7\ \text{s}^{-1}$, compatible with the experimental estimate. On the other hand, we cannot reproduce the very steep increase of the rate constant with temperature reported in Ref. 35. Since such an increase is not observed for the rate constants in neat crystals, discussed in the following section, we have made no further attempt to account for these observations.

E. Rate constants in undoped crystals

In neat benzoic acid crystals, the asymmetry of the potential prevents the observation of tunneling splitting. Double proton transfer can be studied as a rate process down to very low temperatures by NMR relaxometry. At temperatures below 20 K, the magnetic relaxation rate τ_c^{-1} tends to become temperature independent, reaching values of $1.22\times10^8\ \text{s}^{-1}$, $4.5\times10^6\ \text{s}^{-1}$, and $2-3\times10^5\ \text{s}^{-1}$, respectively,[7,8,24] for HH, HD, and DD transfers in powders. Because of the asymmetry of the transfer potential, the rate constants deduced from spin-lattice relaxation times τ_c consist of the sum of an uphill and downhill term, which will differ by a Boltzmann factor corresponding to an energy difference ΔE (of about 60 cm^{-1}):

$$\tau_c^{-1}=k_{\text{down}}+k_{\text{up}}=k_{\text{down}}[1+e^{-\Delta E/k_BT}]. \tag{25}$$

The value for the HH rate constant quoted above, corresponding to $k(0)=k_{\text{down}}$, is at least an order of magnitude larger than that quoted in Sec. V D for HH transfer in crystals doped with thioindigo, which was found to be compatible with the matrix element measured for the splitting. This suggests that the tunneling distance for dimers adjacent to

the dopant is somewhat larger than for unperturbed dimers in the crystal.

To investigate this further, we carried out a direct calculation of the relaxation rate (25) in which k_{down} is represented by a sum of tunneling and classical rate constants of the type (17), each evaluated with parameters modified by the lattice environment. Thus the corresponding instanton action $[S_I(T)]_{\mathrm{solid}}$ can be found if we adopt the compression factor ρ defined by Eq. (20) together with the correcting factors $\Sigma_{s,a}\delta_{s,a}^{\mathrm{lattice}}$ for coupling with the lattice phonons defined by Eqs. (23) and (24) and estimated in Sec. V C. This leads to the replacement of the instanton action (14) in the rate expression (17) by

$$[S_I(T)]_{\mathrm{solid}} = \frac{[S_I^0(T)]_{\mathrm{gas}}\rho}{1+\sum_s^{(\mathrm{LF})}[\delta_s(T)+\delta_s^{\mathrm{lattice}}(T)]} + \alpha\sum_a^{(\mathrm{LF})}[\delta_a(T)+\delta_a^{\mathrm{lattice}}(T)], \tag{26}$$

where $\rho=0.83$, as found in Sec. V C. The same factor is used to represent the dependence of the barrier height on the transfer distance, as required for the evaluation of the classical component $k_{\mathrm{TST}}(T)$ in Eq. (17). The presence of strongly coupled modes with zeta factors (4) close to unity causes some numerical uncertainty. For instance, for HH transfer at zero temperature the calculated rate constant varies from 7.1×10^7 s^{-1} in the (preferred) adiabatic approximation to 3.4×10^7 s^{-1} in the sudden approximation for the modes implicated. These values are in reasonable agreement with the observed low-temperature rate constant of 1.22×10^8 s^{-1}. In Sec. V C we found that the same calculation produced a tunneling splitting twice as large as the observed value. Although both calculations yield results well within the margin of error that may be expected, it is worth noting that the model overestimates the splitting in the doped crystal but underestimates the rate constant in the neat crystal. This supports the tentative conclusion drawn from a direct comparison of the experimental data that the tunneling distance near the dopants exceeds that of the unperturbed dimers in the solid.

A complete set of temperature-dependent rate constants for HH, HD, and DD transfers calculated in the sudden and adiabatic approximation limits, together with their geometric mean, is compared with the reported experimental observations[24] in Fig. 4. For temperatures up to about 150 K, the two approximations yield similar results and reproduce the observed relaxation rates and kinetic isotope effects satisfactorily. At higher temperatures, the calculated rates exceed the observed values, especially for the light isotope, as illustrated in Fig. 5, where the solid lines represent the geometric mean results and the broken lines the high-temperature components $k_{\mathrm{TST}}(T)$. The difference in temperature dependence between the observed and calculated rate constants at high temperatures may mean that the barrier height calculated as $U_A\rho=6.1$ kcal/mol is overestimated by about 0.5 kcal/mol. The formic acid results listed in Table II indicate that the B3LYP barrier is indeed higher than the presumably more accurate MCG3 barrier by such an amount

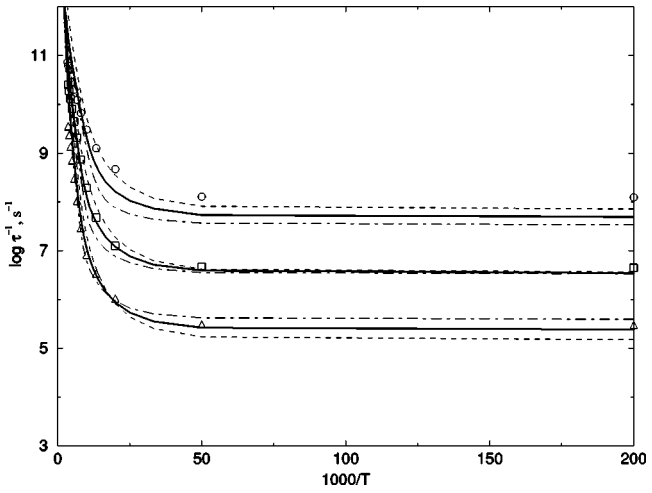

FIG. 4. Comparison of spin-lattice correlation rates measured by NMR relaxometry with those calculated by AIM/DOIT for solid benzoic acid isotopomers with mobile HH (top), HD (center), and DD (bottom) pairs. Measurements taken from Ref. 24 are depicted by symbols. The broken and dot-dashed lines represent calculations in which coupled vibrations with $\zeta \simeq 1$ (see Sec. II) are treated in the adiabatic and sudden approximation, respectively. The solid curve represents the geometric mean of these two results.

(8.38−7.94=0.44 kcal/mol). This suggests that a higher level of calculation such as MCG3 may yield a more satisfactory temperature dependence. On the other hand, a method leading to a lower barrier would tend to yield higher rates. This problem remains to be resolved.

To conclude, we return to the calculated isotope effects for transfer rate constants in the formic acid dimer. In Sec. IV B we reported that our values for these effects were relatively close to those obtained earlier by Kim[31] but much larger than those obtained by Tautermann *et al.*,[32] as illustrated in Fig. 2. The latter authors argued that their smaller-than-expected isotope effects are due to the different zero-

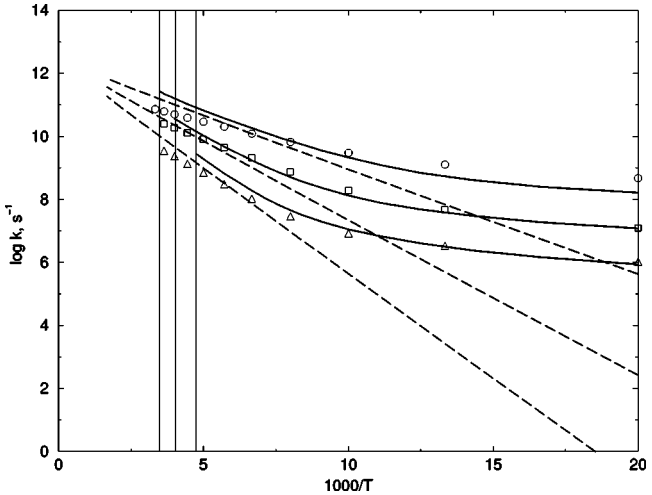

FIG. 5. Expansion of the high-temperature part of Fig. 4. The solid lines are the same as in Fig. 4 but the broken lines represent classical TST rate constants calculated for a barrier height of 6.1 kcal/mol obtained by scaling the B3LYP barrier for the isolated dimer (see Table II) by a compression factor $\rho=0.83$ derived for the solid (see Sec. V C). The vertical lines represent crossover temperatures for, from left to right, HH, HD, and DD transfers.

point energy corrections for HH compared to DD transfer. However, the observed rate constants and kinetic isotope effects for benzoic acid shown in Figs. 4 and 5 contradict this interpretation, because in comparable systems the lower the rate, and thus the higher and/or wider the barrier, the larger should be the isotope effect. We find that couplings between the reaction coordinate and transverse modes are quite similar in the two dimers and so are the zero-point energy corrections. The lower rates in the formic acid dimer compared to the benzoic acid crystal is therefore mainly due to the higher barrier, which implies a larger kinetic isotope effect. The smaller isotope effects calculated in Ref. 32, namely, 61 compared to 360 at 100 K and 10 compared to 17 at 275 K are therefore unlikely to be correct. This implies that the conclusions[32] drawn from them may need revision.

VI. DISCUSSION

A common problem in the interpretation of tunneling splittings in high-resolution spectra is the decomposition of the observed splitting into components of the two states involved in the transition. This problem interfered with the assignments for all three dimers considered in this paper. In the present work we offer a solution based on direct dynamics calculations that allow an interpretation in simple physical terms. In the case of the formic acid dimer, both the problem and the solution are straightforward, the problem because two distinct splittings could be measured and the solution because direct calculations could be carried out on the two levels involved. The calculations produce the unequivocal conclusion, supported by strong symmetry arguments, that the original assignment of the two splittings must be reversed, the larger splitting being a property of the ground state rather than the vibrationally excited state.

For the benzoic acid dimer, where the transition is to an electronically excited state, such a straightforward answer cannot be given, since only a single splitting is observed and since the calculation of tunneling splittings in excited states of such large system remains a very difficult problem. In this case the conclusion that the observed splitting is essentially that of the ground state is based on ground-state calculations only, together with a number of qualitative arguments based on the nature of the excited state. The main argument is that the excitation weakens the hydrogen bonds and renders them nonequivalent. In such a situation, the weaker of the two bonds has the larger influence on the double proton transfer. This was recently demonstrated for the 2-pyridone/2-hydroxypyridine dimer by selective deuteration of the two inequivalent mobile protons.

The hydrogen bonding is stronger in the benzoic than in the formic acid dimer and the tunneling splitting is correspondingly larger. The hydrogen bonding is still stronger for crystalline benzoic acid where the dimers are compressed by crystal forces. Because of the low site symmetry, the tautomeric moieties are no longer equivalent; hence no tunneling splitting is observed. The asymmetry of the tunneling potential can be reduced to a value comparable to the transfer coupling by suitable doping of the crystal, which should restore limited tunneling splitting. Although such a splitting has not yet been observed directly in the solid environment, high-resolution laser spectroscopy has made it possible to measure the corresponding transfer matrix element, whose value roughly corresponds to the splitting for a symmetric potential. NMR relaxometry has made it possible to deduce temperature-dependent transfer rate constants from spin relaxation times in neat crystals. Our calculations offer a unified interpretation of these four pieces of experimental information: the splitting in the gas-phase dimer, the transfer matrix element and the low-temperature limit of the rate constant in the doped crystal, and the transfer rate constant in the neat crystal of benzoic acid. The unification is achieved by inclusion of the effects of crystal forces on the quantum-chemically calculated parameters of the gas-phase dimer. Three effects are directly included: (1) the static compression of the intradimer distance; (2) the dynamic modulation of this distance by the most strongly coupled symmetric lattice phonons; and (3) the Franck–Condon effect of the most strongly coupled antisymmetric lattice phonons. The combined effect, calculated from the observed intradimer distance in the solid, accounts very well for the relationship between the splitting in the gas-phase dimer and the transfer rate constant in the neat crystal. It also accounts for the low-temperature data reported for doped crystals if we assume that the compression of the intradimer distance in dimers adjacent to the dopant is somewhat smaller than that of regular dimers in the lattice.

The same unified approach also accounts satisfactorily for the observed kinetic isotope effects on the rate constants in neat benzoic acid crystals. Earlier,[5] this approach had been found to allow a consistent assignment of the isotope effects on the splitting observed in the 2-pyridone/2-hydroxypyridine dimer, where HD and DH splittings differ. These results have implications for the calculated kinetic isotope effects for rates of transfer in the formic acid dimer; in particular, they suggest that the effects recently obtained by Tautermann *et al.*[32] are too small.

The dynamic effect of the lattice phonons in our calculations differs from the usual heat-bath approach. In the present crystals the proton transfer takes place within the dimers; as a result interdimer phonons that move the monomers in phase are found to have only a weak effect on the transfer rate. The weak heat-bath effect is supported by the weak temperature dependence of the observed rate constants in neat crystals, since such an effect would contribute an additional term to the activation energy. A much stronger effect is produced by phonons that move the two monomers in counterphase, since these phonons modulate the transfer distance. This effect, which is to promote tunneling, runs counter to the heat-bath effect, which provides friction. The good agreement between the calculated and observed rate constants at low temperature supports the conclusion that the modulation effect is dominant.

The method's ability to deal in a precise manner with the effect of individual vibrations on the transfer probability allowed us to assign the splittings observed in the formic acid dimer and to quantify the effect of symmetric lattice phonons on the HH, HD, and DD transfer rates in benzoic acid crystals. However, this ability suffers for those coupled vibra-

tions whose frequency and displacement fall in a critical "intermediate" region where neither the adiabatic nor the sudden approximation limit is appropriate. Such modes happen to contribute to the transfer in both the formic and the benzoic acid dimer. To cope with this problem, we have used a heuristic averaging procedure together with error limits representative of the two limiting approximations. While this affects the numerical accuracy of several of our results, it does not alter the conclusion that a wide range of available data on double proton tunneling in carboxylic acids and related compounds, both in the gas phase and in solids, can be explained in terms of a single multidimensional model.

ACKNOWLEDGMENTS

Z.S. acknowledges the University of Santiago de Compostela, Spain, for a Visiting Professorship in 2004, when this work was initiated. A.F.-R. acknowledges the Ministerio de Ciencia y Tecnologia of Spain for a Ramon y Cajal research contract and for the Research Project No. BQU2003-01639. Computing facilities made available by the Centro de Supercomputacion de Galicia (CESGA) are gratefully acknowledged.

[1]F. Madeja and M. Havenith, J. Chem. Phys. **117**, 7162 (2002).
[2]K. Remmers, W. L. Meerts, and I. Ozier, J. Chem. Phys. **112**, 10890 (2000).
[3]D. R. Borst, J. R. Roscoli, D. W. Pratt, G. M. Florio, T. S. Zwier, A. Müller, and S. Leutwyler, Chem. Phys. **283**, 341 (2002).
[4]Z. Smedarchina, W. Siebrand, A. Fernández-Ramos, and E. Martínez-Núñez, Chem. Phys. Lett. **117**, 396 (2004).
[5]J. R. Roscoli, D. W. Pratt, Z. Smedarchina, W. Siebrand, and A. Fernández-Ramos, J. Chem. Phys. **120**, 11351 (2004).
[6]A. Oppenländer, C. Rambaud, H. P. Trommsdorff, and J.-C. Vial, Phys. Rev. Lett. **63**, 1432 (1989).
[7]A. Heuer and U. Haeberlen, J. Chem. Phys. **95**, 4201 (1991).
[8]D. F. Brougham, A. J. Horsewill, and R. I. Jenkinson, Chem. Phys. Lett. **272**, 69 (1997).
[9]D. F. Brougham, A. J. Horsewill, and H. P. Trommsdorff, Chem. Phys. **243**, 189 (1999).
[10]C. Rambaud and H. P. Trommsdorff, Chem. Phys. Lett. **306**, 124 (1999).
[11]C. C. Wilson, N. Shankland, and A. J. Florence, J. Chem. Soc., Faraday Trans. **92**, 5051 (1996).
[12]L. Leiserowitz, Acta Crystallogr., Sect. B: Struct. Crystallogr. Cryst. Chem. **32**, 775 (1976).
[13]S. Hayashi, J. Imemura, S. Kato, and K. Morokuma, J. Chem. Phys. **88**, 1984 (1984).
[14]Y.-T. Chang, Y. Yamaguchi, W. H. Miller, and H. F. Schaeffer III, J. Am. Chem. Soc. **109**, 7247 (1987).
[15]N. Shida, P. F. Barbara, and J. Almlöf, J. Chem. Phys. **94**, 3633 (1991).
[16]M. E. Neumann, S. Graciun, A. Corval, M. R. Johnson, A. J. Horsewill, V. A. Benderskii, and H. P. Trommsdorff, Ber. Bunsenges. Phys. Chem. **102**, 325 (1998); V. A. Benderskii, E. V. Vetoshkin, S. Yu. Grebenshchikov, L. von Laue, and H. P. Trommsdorff, Chem. Phys. **117**, 119 (1997).
[17]H. Ushiyama and K. Takatsuka, J. Chem. Phys. **115**, 5903 (2001).
[18]M. V. Vener, O. Köhn, and J. M. Bowman, Chem. Phys. Lett. **349**, 562 (2001).
[19]T. Loerting and K. R. Liedl, J. Am. Chem. Soc. **120**, 12595 (1998).
[20]C. S. Tautermann, A. F. Voegele, and K. R. Liedl, J. Chem. Phys. **120**, 631 (2004).
[21]Z. Smedarchina, A. Fernández-Ramos, and W. Siebrand, Chem. Phys. Lett. **395**, 339 (2004).
[22]W. Siebrand, Z. Smedarchina, M. Z. Zgierski, and A. Fernández-Ramos, Int. Rev. Phys. Chem. **18**, 5 (1999).
[23]Z. Smedarchina, A. Fernández-Ramos, and W. Siebrand, J. Comput. Chem. **22**, 787 (2001).
[24]Q. Xue, A. J. Horsewill, M. R. Johnson, and H. P. Trommsdorff, J. Chem. Phys. **120**, 11107 (2004).
[25]R. Meyer and R. R. Ernst, J. Chem. Phys. **86**, 784 (1987); **93**, 5518 (1990).
[26]A. Stöckli, B. H. Meier, R. Kreis, R. Meyer, and R. R. Ernst, J. Chem. Phys. **93**, 1052 (1990).
[27]Z. Smedarchina, W. Siebrand, and M. Z. Zgierski, J. Chem. Phys. **103**, 5326 (1995).
[28]B. J. Lynch and D. G. Truhlar, J. Phys. Chem. A **107**, 3898 (2003), and references therein.
[29]Th. Neuheusser, B. A. Hess, Ch. Reutel, and E. Weber, J. Phys. Chem. **98**, 6459 (1994).
[30]A. Almessingen, O. Bastiansen, and T. Motzfeldt, Acta Chem. Scand. (1947-1973) **23**, 2848 (1969).
[31]Y. Kim, J. Am. Chem. Soc. **118**, 1522 (1995).
[32]C. S. Tautermann, M. J. Loferer, A. F. Voegele, and K. R. Liedl, J. Chem. Phys. **120**, 11650 (2004).
[33]C. S. Tautermann, A. F. Voegele, T. Loerting, and K. R. Liedl, J. Chem. Phys. **117**, 1962 (2002).
[34]M. J. Frisch *et al.*, GAUSSIAN 98, Revision A.11 Gaussian, Inc., Pittsburgh, PA, 1998.
[35]C. Rambaud, A. Oppenländer, M. Pierre, H. P. Trommsdorff, and J.-C. Vial, Chem. Phys. **136**, 335 (1989).
[36]S. Hayashi, M. Oobatake, R. Nakamura, and K. Machida, J. Chem. Phys. **94**, 4446 (1991).
[37]M. Plazanet, N. Fukushima, M. R. Johnson, A. J. Horsewill, and H. P. Trommsdorff, J. Chem. Phys. **115**, 3241 (2001).
[38]A. Almessingen, O. Bastiansen, and T. Motzfeldt, Acta Chem. Scand. (1947-1973) **24**, 747 (1970); M. D. Harmony, V. W. Laurie, R. L. Kuczkowski, R. H. Schwendeman, D. A. Ramsay, F. J. Lovas, W. J. Lafferty, and A. G. Maki, J. Phys. Chem. Ref. Data **8**, 619 (1979).